

Gas-Phase Photooxidation of Trichloroethylene on TiO₂ and ZnO: Influence of Trichloroethylene Pressure, Oxygen Pressure, and the Photocatalyst Surface on the Product Distribution

M. D. Driessen,[†] A. L. Goodman, T. M. Miller, G. A. Zaharias, and V. H. Grassian*

Department of Chemistry, University of Iowa, Iowa City, Iowa 52242

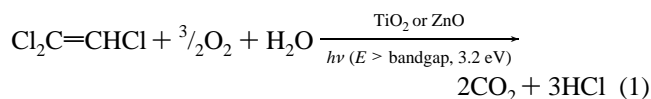
Received: July 18, 1997; In Final Form: November 6, 1997[⊗]

Transmission Fourier transform infrared spectroscopy has been used to identify gas-phase and surface-bound products and intermediates formed during the gas-phase photooxidation of trichloroethylene (TCE) on TiO₂ and ZnO. Several factors are found to influence the gas-phase product distribution for this reaction. On clean TiO₂ and ZnO surfaces and at high TCE and O₂ pressures, gas-phase CO, CO₂, COCl₂, CCl₂HCOCl, CHCl₃, C₂HCl₅, and HCl are produced, whereas at low TCE and O₂ pressures, TCE is converted to gas-phase CO and CO₂ only. In addition to TCE and O₂ pressure, the product distribution of the photooxidation of TCE is strongly dependent upon the coverage of adsorbed species on the surface of the photocatalyst. It is shown here that the complete oxidation of adsorbed TCE can occur on clean photocatalytic surfaces whereas only partial oxidation of adsorbed TCE occurs on adsorbate-covered surfaces. The role of adsorbed surface products in TCE photooxidation is discussed.

Introduction

Trichloroethylene (TCE), a human health hazard, is the most common halogenated contaminant found in groundwater supplies.¹ Therefore, a great deal of effort has been put forth in developing methods to degrade or transform this contaminant into more environmentally benign compounds.^{2–13} Several approaches have been taken; some of the more promising approaches involve the aqueous and gas-phase photooxidation of TCE using semiconductor photocatalysts such as TiO₂.^{2–13} These catalysts are activated by absorption of light with wavelengths contained in the solar spectrum.

Reaction 1 shows the ideal photooxidation reaction where TCE is completely mineralized into CO₂ and HCl. Either adsorbed water or surface-bound hydroxyl groups present on the semiconductor surface may participate in the reaction.



However, the complete mineralization of TCE is often times not realized as other products have been identified in the reaction. Recently, there has been some debate concerning the product distribution and the mechanism of the gas-phase photooxidation of TCE on TiO₂.^{3–13} There are a few studies that report the complete mineralization of TCE during the photooxidation of TCE on TiO₂.^{3–5} However, a greater number of studies that report the formation of chlorinated partial oxidation products such as phosgene, dichloroacetyl chloride (DCAC), monochloroacetyl chloride (MCAC), dichloroacetic acid (DCAA), and monochloroacetic acid (MCAA);^{6–13} some of these compounds are even more toxic than TCE.¹¹ It has

been suggested that differences in product distribution of the photooxidation of TCE on TiO₂ can, in some cases, be attributed to the reaction and hydrolysis of these chlorinated partial oxidation products on the surface of TiO₂ particles that, because of reactor design, are not exposed to light.⁷

In this study, it is shown that gas-phase products formed in the photooxidation of TCE on both TiO₂ and ZnO are dependent upon the reaction conditions employed. The product distribution is found to depend on TCE pressure, O₂ pressure, and the nature of the photocatalyst surface. On clean TiO₂ and ZnO surfaces and under conditions of low pressures of TCE (144 mTorr) and molecular oxygen (721 mTorr), CO and CO₂ are the only carbon-containing, gas-phase products formed. After the reaction is run at low pressure, the catalyst surface is covered with several adsorbed species including water and dichloroacetate. Subsequent photooxidation of TCE on the adsorbate-covered photocatalyst results in the formation of gas-phase CO, CO₂, and additional carbon-containing, gas-phase products. These products include COCl₂, DCAC, C₂HCl₅, CHCl₃, and HCl. At high initial pressures of TCE ($P > 144$ mTorr), CO and CO₂ as well as COCl₂, DCAC, CHCl₃, and C₂HCl₅ are produced in the gas phase when either clean or adsorbate-covered ZnO and TiO₂ photocatalysts are used. As discussed here, the different product distributions for this reaction are caused by changes in the photocatalyst surface due to adsorbed photoproducts.

Experimental Section

The IR cell used in these experiments has been described previously.^{14,15} The cell consists of a 2³/₄ in. stainless steel cube with two differentially pumped barium fluoride windows and a sample holder through which thermocouple and power feed-throughs are connected to a photoetched tungsten sample grid. The sample holder design is such that the sample may be cooled to near liquid nitrogen temperatures and heated resistively up to 1300 K. The temperature is monitored using thermocouple wires spot-welded to the top of the sample grid. The cell is attached to an all stainless steel vacuum chamber through a 2

[†] Present address: Department of Chemistry, Southwest Missouri State University, Springfield, MO 65804.

* To whom correspondence should be addressed.

[⊗] Abstract published in *Advance ACS Abstracts*, December 15, 1997.

ft bellows hose. The vacuum system is pumped using an 80 L/s ion pump after being rough pumped with a turbomolecular pump.

Samples are made by spraying a slurry of the powdered semiconductor (TiO_2 , Degussa P25; ZnO , Aldrich) and deionized water onto a tungsten grid (Buckbee-Mears) which is held at approximately 573 K. A template is used to mask half of the grid so that one side can be coated with the semiconductor powder, and the other side is left blank. Approximately 60 mg of the semiconductor powder is evenly coated onto a $3 \text{ cm} \times 1 \text{ cm}$ area of the grid.

Once the sample is prepared it is mounted inside the IR cell, after which the cell is evacuated. The sample is then resistively heated to 673 K for $2\frac{1}{2}$ h under vacuum and then oxidized at the same temperature by introducing 100 Torr of O_2 into the IR cell for 30 min. After evacuating the sample cell for 15 min, 100 Torr of oxygen is admitted into the cell, and the sample is cooled to room temperature. Once the sample has reached room temperature, the cell is evacuated for several hours or overnight. This cleaning procedure removes adsorbed hydrocarbon impurities, including carbonates, from the surface. The sample contains isolated hydroxyl groups with infrared frequencies of 3715 and 3672 cm^{-1} , in agreement with literature values.¹⁶

The IR cell is then placed on a linear translator inside the sample compartment of a Mattson RS-1 FT-IR spectrometer equipped with a narrowband MCT detector. The linear translator allows each half of the sample grid to be translated into the infrared beam. This permits the investigation of gas-phase and adsorbed species on the photocatalyst surface under identical reaction conditions. Each spectrum was recorded by averaging 1000 scans at an instrument resolution of 4 cm^{-1} . Each absorbance spectrum shown represents a single beam scan referenced to the appropriate single beam scan of the clean photocatalyst or the blank grid prior to gas introduction, unless otherwise noted.

A 500 W mercury lamp (Oriel Corp.) with a water filter was used as the light source in these experiments. The 300 nm long pass filter ($T = 0$ at 300 nm) was placed in front of the lamp. The broadband light was then reflected off of an aluminum-coated mirror and then turned by a 1 in. quartz prism onto the sample. The quartz prism is mounted inside of the FT-IR sample compartment so that the dry air purge was not broken during irradiation. The power at the sample was measured before each experiment and was typically 190 mW/cm^2 . The temperature of the sample did not exceed 325 K during these experiments.

TCE (Aldrich, 99+%) and DCAC (Aldrich, 99%) were transferred to a glass sample bulb and subjected to several freeze-pump-thaw cycles before use. Hydrogen (Air Products, Research Grade) and oxygen (Air Products, 99.6%) were used as received. Gas pressures were initially measured in a volume of 823 mL and then expanded into the infrared cell, which is an additional 320 mL in volume. A valve between these two portions of the vacuum chamber was then closed before irradiation so that the total amount of reactants available in the infrared cell are the pressures specified in the text contained in the 320 mL volume of the infrared cell.

Results

TCE Adsorption on TiO_2 and ZnO at Room Temperature.

The infrared spectrum of adsorbed TCE as a function of TCE pressure on TiO_2 is shown in Figure 1. Gas-phase contributions to the spectra shown in Figure 1 have been subtracted out. After

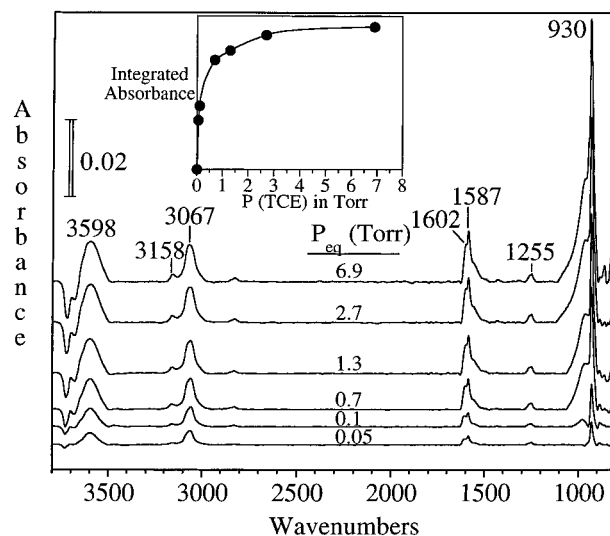


Figure 1. Infrared spectra of TCE adsorbed on TiO_2 as a function of TCE pressure. The inset displays a plot of the integrated area of the 930 cm^{-1} band of adsorbed TCE as a function of TCE pressure. The data show that the TiO_2 surface saturates above a TCE pressure of approximately 1.4 Torr.

TABLE 1: Vibrational Assignment of TCE Adsorbed on TiO_2 (All Values in cm^{-1})

mode description ^a	gas-phase TCE ^b	adsorbed TCE on TiO_2 ^b	adsorbed TCE on ZnO ^b
$2\nu(\text{C}=\text{C})$	3168	3158	
$\nu(\text{CH})$	3096	3067	3085
$2\nu(\text{C}-\text{Cl})$		1602	1602
$\nu(\text{C}=\text{C})$	1575	1587	1586
$\delta(\text{CHCl})$	1254	1255	1254
$\nu(\text{C}-\text{Cl})$	940	930	935
$\nu(\text{C}-\text{Cl})$	848	n.o. ^c	845
$\nu(\text{C}-\text{Cl})$	783	n.o. ^c	782

^a Mode description taken from ref 18. ^b This work. ^c n.o. = not observed, below absorptions of TiO_2 .

introduction of gas-phase TCE into the IR cell, bands due to adsorbed TCE are observed near 3158, 3067, 1602, 1587, 1255, and 930 cm^{-1} . The intensities of these bands increase with increasing TCE pressure until the TiO_2 surface becomes saturated at equilibrium pressures greater than 1.4 Torr (see inset of Figure 1). The vibrational bands of adsorbed TCE can be assigned by comparison with the vibrational spectrum of gas-phase TCE (Table 1). A shift of 12 cm^{-1} to higher frequencies is observed for the $\text{C}=\text{C}$ stretching mode, along with shifts to lower frequencies of the $\text{C}-\text{H}$ and $\text{C}-\text{Cl}$ stretching modes. Hydrogen bonding is observed as a loss in intensity of the $\nu(\text{OH})$ band near 3715 and 3672 cm^{-1} for free hydroxyl groups on the TiO_2 surface with a concomitant growth in the associated hydroxyl stretching region near 3598 cm^{-1} . There are probably several sites for adsorption of TCE on the TiO_2 surface. The IR data show that there is some interaction between TCE and the OH groups on the TiO_2 surface.

Infrared data obtained for the adsorption of TCE on ZnO show much less TCE adsorption on ZnO compared to TiO_2 . This in part can be attributed to the substantial difference in the surface areas of ZnO and TiO_2 (the ZnO particles used in these studies have an estimated surface area of approximately $5 \text{ m}^2/\text{g}$ whereas Degussa P25 TiO_2 has a surface area near $50 \text{ m}^2/\text{g}$) and in part to a weaker interaction of TCE with ZnO . At high pressures (greater than 1.4 Torr) where TCE adsorption saturates on the surface of TiO_2 , small infrared absorptions due

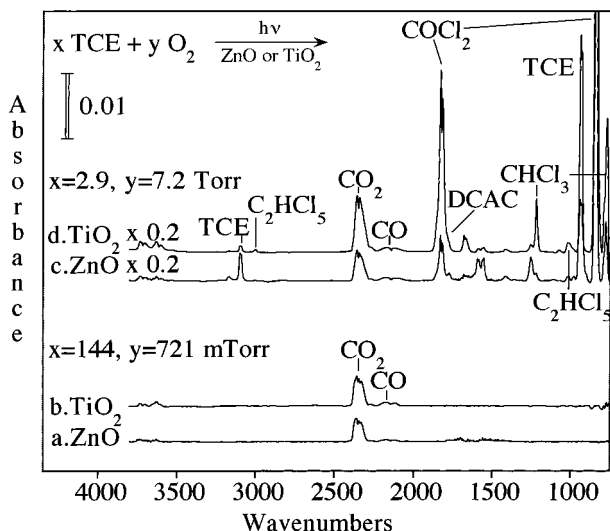


Figure 2. Infrared spectra recorded of the gas phase during the photooxidation of TCE. The spectra labeled a and b show gas-phase absorptions following irradiation of 144 mTorr of TCE and 721 mTorr of O₂ on clean ZnO and TiO₂, respectively. The spectra labeled c and d show gas-phase absorptions following irradiation of 2.9 Torr of TCE and 7.2 Torr of O₂ on ZnO and TiO₂, respectively. These spectra show the product distribution of the photooxidation of TCE on both clean ZnO and TiO₂ is dependent upon the reaction conditions employed.

to adsorbed TCE on ZnO are observed. The frequencies of these absorptions are given in Table 1.

Photooxidation of TCE on Clean TiO₂ and ZnO Surfaces.

Figure 2 displays the infrared spectra of the gas-phase photooxidation products following irradiation of two different reaction mixtures of TCE and O₂ on both ZnO and TiO₂. The gas-phase infrared spectra taken following photooxidation of TCE on ZnO and TiO₂, starting with 144 mTorr of TCE and 721 mTorr of O₂, are shown in parts a and b, respectively. Gas-phase infrared absorption bands due to photooxidation products with frequencies near 2147 and 2349 cm⁻¹ are observed and assigned to gas-phase CO and CO₂, respectively. Under these conditions, complete conversion is achieved in 2 min on TiO₂ and 20.5 h on ZnO.

The infrared spectra shown in parts c and d of Figure 2 were recorded following the photooxidation of TCE on ZnO and TiO₂, respectively, starting with 2.9 Torr of TCE and 7.2 Torr of O₂. Several infrared absorption bands due to gas-phase species are observed near 3001, 2349, 2144, 1827, 1794, 1677, 1413, 1220, 1076, 1013, 992, 853, and 776 cm⁻¹. From IR standards and literature data,^{9,19-21} these infrared absorption bands can be assigned to a combination of the following: COCl₂, DCAC, CO, CO₂, CHCl₃, and C₂HCl₅ (see Table 2) with the exception of the band at 1413 cm⁻¹, which is left unassigned. CHCl₃ and C₂HCl₅ have some spectral overlap, and therefore, some of the same bands (1220 and 776 cm⁻¹) are assigned to both of these molecules. Additional absorptions are present in the infrared spectra due to unreacted parent TCE (85% conversion of TCE on TiO₂ after 3 h of irradiation and 40% conversion on ZnO after 21.5 h of irradiation). These data illustrate how the reactant pressures can influence the product distribution for this reaction. They also illustrate that similar processes occur on ZnO and TiO₂.

The wavelength dependence of the photooxidation of TCE was investigated on TiO₂ and ZnO. Figure 3 displays a plot of integrated area of the infrared band for gas-phase CO₂ as a function of the wavelengths used during irradiation. Starting with the longest wavelength first, the ZnO was irradiated for

TABLE 2: Vibrational Assignment of Gas-Phase Products from TCE Photooxidation on TiO₂ and ZnO

obsd freq (cm ⁻¹) ^a	assigned species	mode description
3001	C ₂ HCl ₅ ^e	$\nu(\text{C-H})$
2885 (envelope center)	HCl	$\nu(\text{H-Cl})$
2349	CO ₂	$\nu(\text{C=O})$
2144	CO	$\nu(\text{CO})$
1827	COCl ₂ ^b	$\nu(\text{C=O})$
1794	Cl ₂ HCCOCl (DCAC) ^c	$\nu(\text{C=O})$
1677	COCl ₂ ^b	$2\nu(\text{C-Cl}_2)$
1220	C ₂ HCl ₅ ^e	$\delta(\text{CH})$
1220	CHCl ₃ , ^d C ₂ HCl ₅ ^e	$\delta(\text{CH})$
1076	Cl ₂ HCCOCl (DCAC) ^c	$\nu(\text{C-C})$
1013	C ₂ HCl ₅ ^e	$\nu(\text{C-C})$
992	Cl ₂ HCCOCl (DCAC) ^c	$\nu(\text{C-C})$
853	COCl ₂ ^b	$\nu(\text{C-Cl}_2)$
776	CHCl ₃ , ^d C ₂ HCl ₅ ^d	$\nu_{\text{as}}(\text{CCl}_3)$

^a This work. ^b Reference 19. ^c Reference 20. ^d Reference 9. ^e Reference 21.

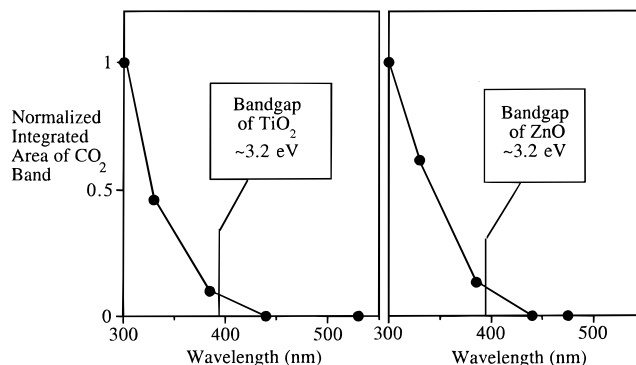


Figure 3. Plot of the normalized integrated area of the infrared band for gas-phase CO₂ following irradiation of TCE on TiO₂ (left) and ZnO (right) as a function of wavelength. Broadband filters were used in these experiments, and the data points plotted are at the cutoff wavelength for each filter used.

10 min. The next longest wavelength filter was then put in place, and irradiation was continued for an additional 10 min. This procedure was followed for all five filters used in this experiment. The increase in integrated area of the CO₂ infrared band after irradiation with each filter was then corrected for differences in light output between filters. The TiO₂ wavelength dependence was determined in a similar manner. As can be seen, the onset wavelength of CO₂ production coincides with the bandgap of TiO₂ and ZnO, and at shorter wavelengths, above the bandgap, CO₂ production increases even more. The wavelength dependence indicates that the photooxidation of TCE is initiated by the excitation of the photocatalyst and not by direct absorption of TCE, which absorbs UV light with $\lambda < 250$ nm.¹⁷

Photooxidation of TCE on Adsorbate-Covered TiO₂ Surfaces. The infrared spectra shown in Figure 2 provide clear evidence that gas-phase COCl₂, DCAC, and CHCl₃ do not form under conditions of low TCE and O₂ pressure on clean ZnO and TiO₂ samples; however, chlorinated partial oxidation products do form at low pressures of TCE and O₂ on used TiO₂ samples. Figure 4 displays the gas-phase infrared spectra following the successive irradiation of 144 mTorr of TCE in the presence of 721 mTorr of oxygen on TiO₂ for 5 min. Each successive run was performed without cleaning the TiO₂ sample in between; however, the IR cell was evacuated, and a fresh reactant mixture (TCE and O₂) was introduced before each run. Initially, the only gas-phase product absorptions are found near 2147 and 2349 cm⁻¹ (Figure 4a), corresponding to the formation of CO and CO₂, respectively. Other infrared bands that are

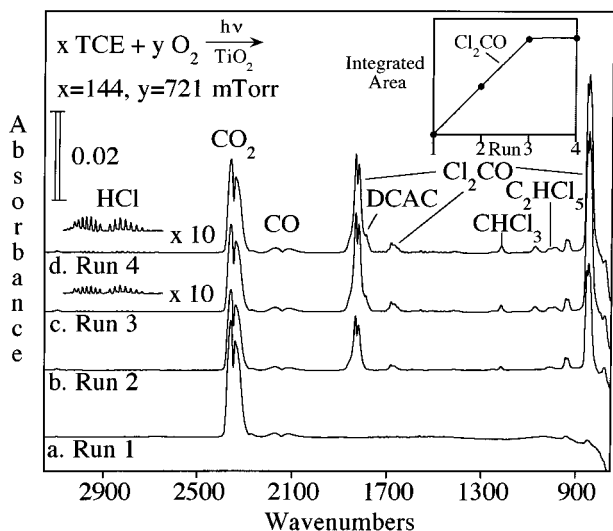


Figure 4. Infrared spectra of the gas phase during the photooxidation of 144 mTorr of TCE and 721 mTorr of O₂. Four successive experiments were performed on the same TiO₂ sample. Initially, for run 1, CO and CO₂ are the only two gas-phase products. Other products are formed in successive runs, runs 2–4. The infrared absorption bands can be assigned to the following gas-phase products: CO₂, CO, Cl₂CO, DCAC, CHCl₃, C₂HCl₅, and HCl (see Table 2). The inset shows that the amount of phosgene produced after each run eventually levels off.

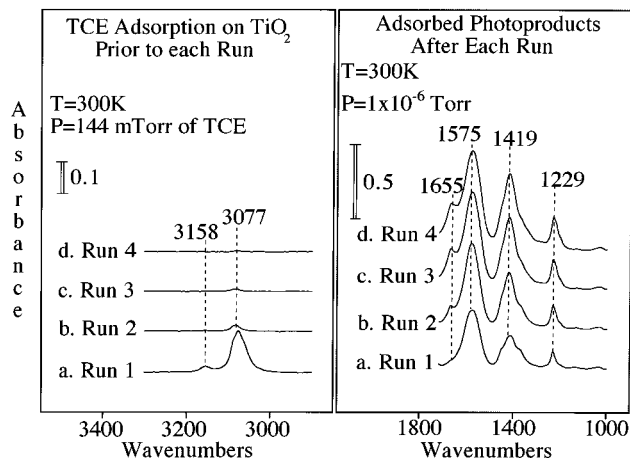


Figure 5. Right panel: infrared spectra of the adsorbed photoproducts on TiO₂ following each of the successive runs shown in Figure 4 (runs 1–4). Left panel: infrared spectra of adsorbed TCE prior to each of the successive runs shown in Figure 4 (runs 1–4). The amount of TCE that can adsorb prior to each run decreases as the coverage of adsorbed products increases.

seen in the spectrum (e.g., at 942 cm⁻¹) are due to unreacted parent TCE. After 5 min of irradiation, approximately 85% of the TCE has been consumed in each of the runs. Successive runs (runs 2–4) show the appearance and growth of several new infrared absorptions. A progression of bands near 2885 cm⁻¹ becomes apparent after runs 3 and 4. These bands correspond to the rovibrational spectrum of HCl. Other absorption bands near 2349, 2144, 1827, 1794, 1677, 1413, 1220, 1076, 1013, 992, 853, and 776 cm⁻¹ are also observed in runs 2–4. As before, it is possible to identify these gas-phase products from their infrared absorptions as CO₂, CO, COCl₂, DCAC, CHCl₃, C₂HCl₅, and HCl (Table 2).

Infrared spectra of the TiO₂ surface were also recorded after each of the four runs. These spectra are shown in the right panel of Figure 5. After run 1, infrared absorptions due to surface-bound species are observed near 1655, 1575, 1456

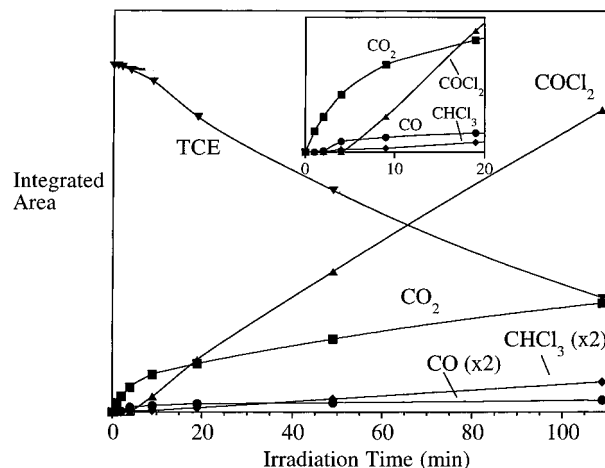


Figure 6. Integrated absorbance of infrared bands for the specified gas-phase products from the photooxidation of 2.9 Torr of TCE and 7.2 Torr of O₂ on TiO₂ as a function of irradiation time. The inset displays an enlarged view of the first 20 min of irradiation.

(shoulder), 1419, 1375 (shoulder), and 1229 cm⁻¹. These spectra show that the titania surface becomes nearly saturated with adsorbed species by the third run as there is almost no change in the infrared bands associated with the surface-bound species between runs 3 and 4 (Figure 5, c and d). There is clearly a correlation between the infrared data for gas-phase and surface-bound products. The infrared data show that COCl₂, DCAC, C₂HCl₅, CHCl₃, and HCl are produced in increasing amounts as the TiO₂ surface becomes more saturated with adsorbed species. The production of phosgene is seen to reach a plateau after three runs (see inset Figure 4) where the TiO₂ surface has become saturated with adsorbed species.

A consequence of the accumulation of surface-bound products on the TiO₂ surface is that the amount of TCE that adsorbs on the TiO₂ surface decreases before each run. This is illustrated in the left panel of Figure 5. The infrared spectra of adsorbed TCE prior to runs 1–4 are shown. The spectra show that, after the initial photooxidation of 144 mTorr of TCE; there is a substantial decrease in the amount of adsorbed TCE; the integrated area of the TCE absorption band in the C–H stretching region shows that less than 10% of the initial amount of adsorbed TCE can adsorb (Figure 5, left panel). Following run 2 (Figure 5c), less than 1% of the initial amount of TCE can adsorb due to the buildup of adsorbed photoproducts on the catalyst surface. It is clear from the data presented in Figure 5 that adsorbed photoproducts block surface sites so that the amount of adsorbed TCE decreases following each run.

The influence of adsorbed species on the TiO₂ surface on the gas-phase product distribution is also evident in the higher pressure reaction. Figure 6 shows the integrated area of the infrared bands due to several gas-phase products (CO₂, CO, COCl₂, and CHCl₃) formed during the photooxidation of 2.9 Torr of TCE with 7.2 Torr O₂ on initially clean TiO₂ plotted as a function of irradiation time. The inset shows an expanded view of the irradiation time between 0 and 20 min. The plot shows that the product distribution changes over time. The inset shows that only CO and CO₂ are formed in the first 5 min of reaction. At later times phosgene and chloroform are formed as well. The induction period for chlorinated partial-oxidation products can be correlated with the buildup of adsorbed surface products from the photooxidation of TCE; i.e., only after some critical surface coverage of adsorbed products is reached are chlorinated products formed.

The spectrum recorded of the TiO₂ surface after photooxi-

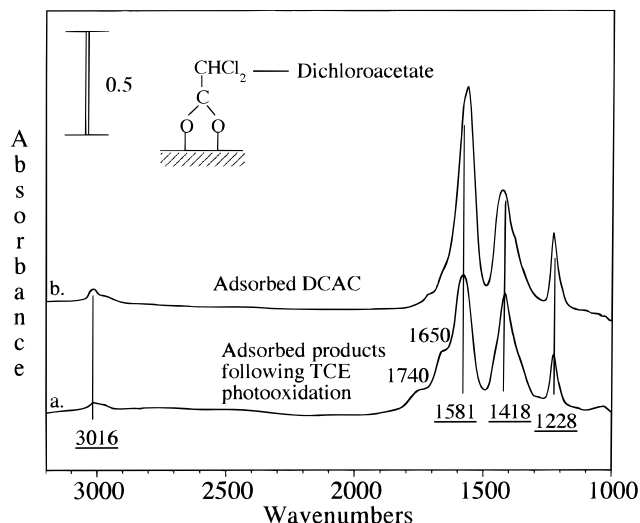


Figure 7. (a) Infrared spectrum of the TiO₂ photocatalyst following photooxidation of 2.9 Torr of TCE in the presence of 7.2 Torr of O₂. (b) Infrared spectrum of TiO₂ following adsorption of DCAC. The frequencies of the bands that are underlined are assigned to adsorbed dichloroacetate. See text for further discussion.

TABLE 3: Vibrational Assignment of Adsorbed Photoproduct Dichloroacetate (Cl₂HCCO₂) from TCE Photooxidation on TiO₂ (All Values in cm⁻¹)

dichloroacetate-TiO ₂ ^a	mode assignment
3011	$\nu(\text{C-H})$
1581	$\nu_{\text{as}}(\text{COO})$
1418	$\nu_{\text{s}}(\text{COO})$
1228	$\delta(\text{CHCl}_2)$

^a From adsorption of dichloroacetyl chloride on TiO₂. ^b Mode assignments are based on comparison to literature spectra of carboxylates (see ref 23).

dation of TCE at high pressures (2.9 Torr of TCE with 7.2 Torr O₂) is shown in Figure 7a. There are several bands apparent in the spectrum due to adsorbed photoproducts. The assignment of the surface-bound products on the TiO₂ surface is more complicated than the identification of gas-phase products. The frequencies of the infrared bands observed between 1000 and 1800 cm⁻¹ are in the region where carbonate, carboxylate, and water absorptions occur.²²⁻²⁵ Each band in the spectrum is quite broad and may be comprised of several absorption bands. It has been recently determined from NMR studies that the predominant carbon-containing, surface-bound product from TCE photooxidation on TiO₂ is dichloroacetate.²⁶ It was postulated that dichloroacetate formed from the reaction of dichloroacetyl chloride and hydroxyl groups to yield HCl and dichloroacetate. The IR spectrum of the TiO₂ surface following TCE photooxidation at high pressures is consistent with an adsorbed carboxylate.²³ To confirm that dichloroacetate is a surface-bound photoproduct, the surface chemistry of DCAC on TiO₂ was investigated.

The infrared spectrum recorded following adsorption of DCAC on a clean TiO₂ surface is shown in Figure 7b. DCAC was introduced into the IR cell at a pressure of 0.500 Torr and then evacuated. The two spectra shown in Figure 7—the photoproduct spectrum and the DCAC spectrum—are very similar and show that dichloroacetate is a surface-bound product formed during TCE photooxidation. Absorptions near 3016, 1580, 1420, and 1229 cm⁻¹ are associated with dichloroacetate. Additional bands at 1650 and 1740 cm⁻¹ present in the photoproduct spectrum shown in Figure 7a are assigned to the bending mode of adsorbed water and the C=O stretch of an

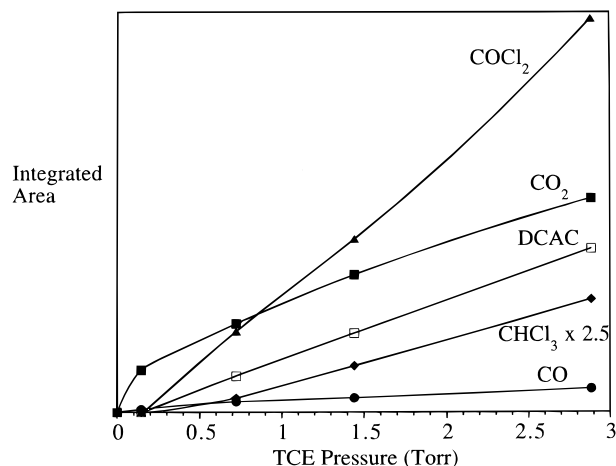


Figure 8. Plot of the integrated area of the infrared absorptions for gas-phase products formed from the photooxidation of TCE on TiO₂ as a function of initial TCE pressure.

adsorbed carbonyl on the TiO₂ surface, respectively. The adsorbed carbonyl is most likely adsorbed phosgene.⁹ The main bands in the photoproduct spectrum have shoulders, this may be due to the presence of other adsorbates of the form CO_x, including CO₂⁻, HCO₂⁻, CO₃²⁻, and HCO₃⁻.

TCE Photooxidation as a Function of O₂ and TCE Pressure. The data presented in Figure 1 show that the product distribution of the photooxidation reaction of TCE changes as a function of the partial pressures of the reaction mixture (TCE and O₂). To further investigate this pressure dependence, experiments were performed as a function of TCE and O₂ pressure. Figure 8 shows a plot of the integrated area of the photooxidation products of TCE versus initial pressure of TCE, in the presence of 7.2 Torr of molecular oxygen. In each case, 7.2 Torr of O₂ is more than the stoichiometric amount needed for complete oxidization of TCE, with the exception of the 2.9 Torr of TCE in which case it is exactly the required pressure to fully oxidize the TCE present. The data shown were collected from the same titania sample that was cleaned between experiments according to the procedure outlined in the Experimental Section. In each case more than 85% of the initial TCE was converted to products. The distribution of products from TCE photooxidation is strongly dependent upon the initial amount of TCE present. It is only at the higher pressures of TCE, at 721 mTorr and above, that detectable amounts of phosgene, DCAC, HCl (not plotted), and CHCl₃ are produced.

Figure 9 displays a plot of the ratio of the integrated areas of the infrared absorptions for two gas-phase photooxidation products of TCE photooxidation, CHCl₃ and CO, plotted as a function of oxygen pressure used. Each experiment was done on an adsorbate saturated sample using 144 mTorr of TCE. This plot illustrates that the product distribution of the photooxidation of TCE is also highly dependent upon oxygen pressure once the surface is saturated with adsorbed species.

Discussion

From the data presented here, it has been shown that, in the presence of molecular oxygen, TiO₂ and ZnO are effective in the photooxidation of TCE using light of wavelengths 390 nm > λ > 300 nm. Differences in the rate of conversion of TCE on TiO₂ relative to ZnO are in part related to differences in the surface area of the two samples used (50 m²/g vs 5 m²/g), although, a full study of the differences in the kinetics of TCE photooxidation on TiO₂ and ZnO has not been done. The TiO₂

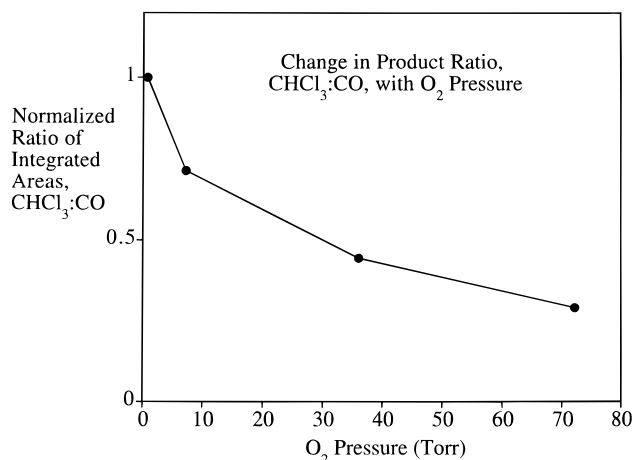


Figure 9. Plot of the ratio of the integrated area of the infrared absorption bands of gas-phase CHCl_3 and CO formed during the photooxidation of TCE on TiO_2 as a function of oxygen pressure. The amount of CO increases relative to CHCl_3 as the oxygen pressure increases.

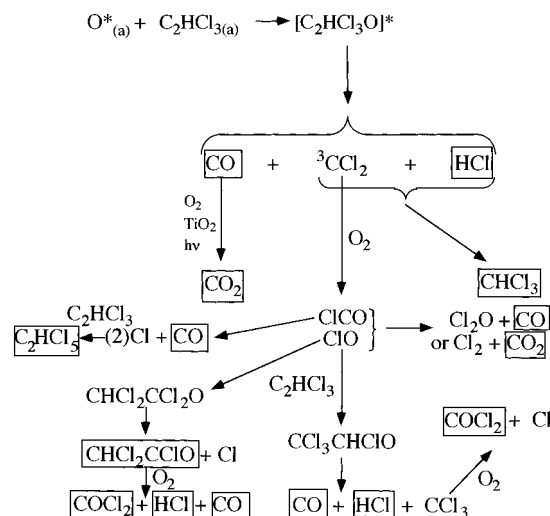
and ZnO data show that the reaction conditions influence product distribution in this reaction. Factors that influence TCE photooxidation are discussed in detail below. Based on the data presented here, a reaction mechanism for TCE photooxidation is given.

Proposed Reaction Mechanisms for TCE Photooxidation on TiO_2 and ZnO . As discussed in the Introduction section, there have been several studies of the gas-phase photooxidation of TCE on TiO_2 .^{3–13} A number of different mechanisms and reactive species have been proposed for this reaction. Nimlos et al. propose that because several of the photooxidation products detected contained more Cl atoms than the parent, Cl atoms must be responsible for the chain propagation of the photooxidation of TCE.¹² Nimlos et al.⁶ have raised the question as to whether some of the reactions that occur during TCE photooxidation over TiO_2 occur in the gas phase or on the TiO_2 surface itself. Fan and Yates suggest that an excited adsorbed oxygen species forms and reacts directly with adsorbed TCE to form DCAC. DCAC can then undergo continued photooxidation to yield COCl_2 .⁹ Phillips and Raupp propose a mechanism that includes hydroxyl and hydroperoxide radicals as the chain propagators.⁸ Hydroxyl radicals as the primary reactive species have also been discussed by Anderson and co-workers.¹³

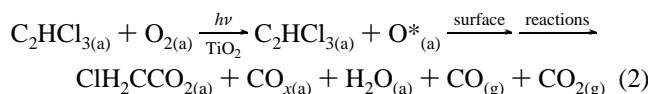
It is clear from the above discussion that there are several different proposals for the identity of the reactive species which initiates the photooxidation of TCE. Here we propose a mechanism that encompasses all of these as contributing to the photooxidation of TCE over TiO_2 . It is proposed that the TCE photooxidation mechanism depends on the coverage of adsorbed products and the availability of surface sites and hydroxyl groups.

Since the initial conditions used in these experiments are similar to those used by Fan and Yates, it is proposed that the initial step in the photooxidation is the excitation of adsorbed oxygen, as they do. The identity of the reactive oxygen species is not known, but for purposes of this discussion, the reactive oxygen species will be represented as O^* without specifying molecular or atomic oxygen. The next step involves reaction O^* with adsorbed TCE. On a clean surface, surface reactions involving O^* and adsorbed chlorinated partial oxidation products continue until the surface is covered with adsorbed products. CO_2 and CO are the only two gas-phase, carbon-containing products formed. This reaction sequence (reaction 2), although

SCHEME 1: Proposed TCE Photooxidation Mechanism on an Adsorbate Covered Surface

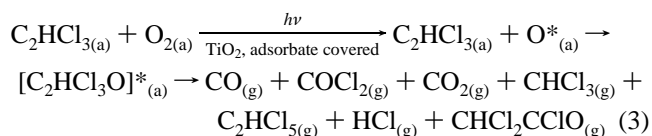


not well understood, requires available surface sites for the complete photooxidation of TCE.



As the surface becomes covered with adsorbed photoproducts, the reaction probability of continued surface reactions decreases. Although the TiO_2 surface is covered with adsorbed photoproducts, the photooxidation of TCE still proceeds, but the products are different; they are in fact the same products observed in the homogeneous gas-phase photooxidation of TCE.^{27–29}

On an adsorbate-covered TiO_2 surface, it is proposed that the initial photooxidation step occurs on the surface, but subsequent chemistry differs. Initially, O^* reacts with TCE to form $[\text{C}_2\text{HCl}_3\text{O}]^*$, an excited adduct (reaction 3).

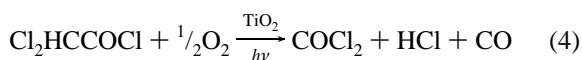


$\text{C}_2\text{HCl}_3\text{O}^*$ has been postulated to form in the homogeneous gas-phase photooxidation of TCE with $\text{O}(^3\text{P})$ and is most likely a diradical with the oxygen bonded to the more positive end of the TCE molecule, making the C–C bond predominantly σ in nature.²⁷ $\text{C}_2\text{HCl}_3\text{O}^*$ is unstable and breaks down to yield reactive species similar to that which forms in the gas phase. A mechanism that accounts for all of the observed species is shown in Scheme 1.^{27–29} The reaction mechanism shown in Scheme 1 is essentially the same as the mechanism proposed for the homogeneous gas-phase photooxidation of TCE.^{27–29} One additional reaction that has been added to Scheme 1 involves the photooxidation of CO on TiO_2 to form gas-phase CO_2 . The gas-phase photoproducts detected in this study are marked with a box.

Chlorine atoms are produced in this reaction mechanism. Cl atoms can undergo reaction with TCE as discussed previously by Nimlos et al.⁹ Although Nimlos et al. have suggested that Cl atoms are the active species in the photooxidation of TCE on TiO_2 , it is not clear how they may be produced to initiate the reaction. Here it is suggested that chlorine atoms are formed through the decomposition of $[\text{C}_2\text{HCl}_3\text{O}]^*$ (Scheme 1) and then

can initiate further photooxidation of TCE, as is observed in gas-phase reactions. The products for the gas-phase, chlorine-initiated oxidation of TCE are DCAC, COCl₂, CHCl₃, and CO,³⁰ similar to the products observed in this study for the photooxidation of TCE on TiO₂ at high pressures. It is also clear from Scheme 1 why quantum yields greater than one have been measured for this reaction, as atomic chlorine is produced in several steps and chlorine atom initiated oxidation is a radical mechanism. Experiments done to trap chlorine atoms and other radical species in the gas phase were unsuccessful, suggesting that the radical mechanism occurs on the surface.³¹

Side reactions of DCAC and phosgene also occur in addition to the reactions shown in Scheme 1. Fan and Yates have demonstrated that DCAC is a reaction intermediate that can undergo continued photooxidation on TiO₂ to yield COCl₂, CO, and HCl (reaction 4).⁹



It has also been established that phosgene reacts with TiO₂ surfaces in the dark to undergo hydrolysis to yield HCl and CO₂. The surface hydrolysis reaction of phosgene to form CO₂ is therefore dependent on the amount of adsorbed water or hydroxyl groups present on the TiO₂ surface.

The role of hydroxyl groups on the TiO₂ surface in the hydrolysis of phosgene was investigated here. A TiO₂ sample that had been previously used as a photocatalyst was cleaned of surface-bound products as described in the Experimental Section. The infrared spectrum of the sample showed that approximately 50% of the surface hydroxyl groups had reacted. This dehydroxylated sample was then used to photooxidize 144 mTorr of TCE in the presence of O₂. The infrared spectrum of the TiO₂ surface following the photooxidation reaction showed a band due to adsorbed phosgene at 1740 cm⁻¹. This same photooxidation was performed on a TiO₂ surface that contained a significant portion of hydroxyl groups, and neither adsorbed (1740 cm⁻¹) nor gas-phase (1827 cm⁻¹) phosgene was observed. The formation of adsorbed phosgene before saturation of the TiO₂ surface with adsorbed products supports a surface-mediated hydrolysis reaction with adsorbed OH groups on the surface of clean TiO₂.

The participation of hydroxyl groups does not imply that hydroxyl radicals are the active species that initiate the photooxidation of gas-phase TCE under the reaction conditions used in this study as Phillips and Raupp⁸ and also Anderson and co-workers¹³ have proposed. Fan and Yates have shown that, under similar reaction conditions as the ones used here, adsorbed H₂O and hydroxyl groups are not the active species that initiate the photooxidation of TCE but are involved in further reactions of adsorbed species.⁹

Influence of Adsorbed Products and Initial Partial Pressures of TCE and O₂. The data presented here clearly demonstrate that the product distribution of TCE photooxidation is dependent upon the surface coverage of adsorbed products. The data herein support the postulated mechanisms showing that the photooxidation occurs initially on the TiO₂ surface to produce only gas-phase CO and CO₂. As the photooxidation proceeds, active sites on the surface of the TiO₂ become covered with adsorbed photooxidation products. The dominant reaction pathway changes from one that occurs on the TiO₂ surface to produce only gas-phase CO and CO₂ as the primary carbon-containing photooxidation products to one that produces several chlorinated products in addition to gas-phase CO and CO₂.

Changes in the TiO₂ surface due to TCE photooxidation have been observed by Larson and Falconer.³² Using post-photo-

oxidation temperature-programmed desorption (TPD), they identified changes in the surface chemistry between fresh TiO₂ catalysts and used or completely deactivated TiO₂ catalysts. They found that a greater amount of CO and CO₂ desorbed from used catalysts during TPD than from fresh TiO₂. They postulated that this was due to the decomposition of larger adsorbates formed from the photooxidation of TCE. It was also proposed that DCAC was an intermediate in the photooxidation of TCE, and therefore the effect of DCAC adsorption on TiO₂ samples was also investigated. Larson and Falconer found that the decomposition of DCAC on the TiO₂ surface decreased the number of adsorption sites and caused the loss in activity of the TiO₂ photocatalyst.³² The infrared data presented here show that a stable product, dichloroacetate, forms on the surface from reaction of DCAC with TiO₂.

There is a product distribution dependence on the TCE pressure. This dependence correlates with the buildup of surface-bound products from the photooxidation of TCE. The higher the initial pressure of TCE, the higher the ratio of gas-phase chlorinated partial-oxidation products relative to CO₂ (see Figure 8). The data in Figure 9 show that the photooxidation of TCE on TiO₂ also has a strong dependence on O₂ pressure. At low pressures of oxygen, there is a larger probability that the CCl₂ radical and HCl will react to form CHCl₃. At higher oxygen pressures, CCl₂ has a higher probability of reacting with a molecule of oxygen to go on to form COCl₂, CO, and HCl, as shown in Scheme 1.

Conclusions

The data presented here show that the photooxidation of TCE on ZnO and TiO₂ is a complicated process. The product distribution can be influenced by several factors including the initial pressures of TCE and molecular oxygen and the adsorbate coverage on the photocatalyst surface. When certain reaction conditions are employed, in particular, low pressures of TCE and clean photocatalyst surfaces, CO and CO₂ are produced as the only two carbon-containing gas-phase products. Additional gas-phase products form at higher initial pressures of TCE and an adsorbate covered photocatalyst surfaces (dichloroacetate and adsorbed water). Two photooxidation mechanisms are proposed to explain these observations. One mechanism involves a multistep surface reaction sequence that can occur on a clean photocatalyst surface to produce predominantly two gas-phase products CO and CO₂. The second mechanism involves a complex series of reactions that follows the mechanism for the homogeneous gas-phase photooxidation of TCE. This second mechanism results in the formation of gas-phase COCl₂, DCAC, CHCl₃, C₂HCl₅, HCl, CO, and CO₂ as well as chlorine atoms that can further initiate photooxidation of TCE.

Acknowledgment. The authors gratefully acknowledge the National Science Foundation (Grant CHE-9614134) for support of this work.

References and Notes

- (1) Dyksen, J. E.; Hess, A. F., III *J. Am. Water Works Assoc.* **1982**, *74*, 394.
- (2) Kenneke, J. F.; Ferry, J. L.; Glaze, W. H. *Photocatalytic Purification and Treatment of Water and Air*; Ollis, D. F., Al-Ekabi, H., Eds.; Elsevier Science Publishers: Amsterdam, 1993; p 179.
- (3) Yamazaki-Nishida, S.; Nagano, K. J.; Phillips, L. A.; Cervera-March, S.; Anderson, M. A. *J. Photochem. Photobiol. A: Chem.* **1993**, *70*, 95.
- (4) Dibble, L. A.; Raupp, G. B. *Catal. Lett.* **1990**, *4*, 345.
- (5) Pruden, A. L.; Ollis, D. F. *J. Catal.* **1983**, *82*, 404.

- (6) Nimlos, M. R.; Jacoby, W. A.; Blake, D. M.; Milne, T. A. *Environ. Sci. Technol.* **1993**, *27*, 732.
- (7) Jacoby, W. A.; Nimlos, M. R.; Blake, D. M.; Noble, R. D.; Koval, C. A. *Environ. Sci. Technol.* **1994**, *28*, 1661.
- (8) Phillips, L. A.; Raupp, G. B. *J. Mol. Catal.* **1992**, *77*, 297.
- (9) Fan, J.; Yates, J. T., Jr. *J. Am. Chem. Soc.* **1996**, *118*, 4686.
- (10) Lichtin, N. N.; Avudaithai, M. *Environ. Sci. Technol.* **1996**, *30*, 2014.
- (11) Jardim, W. F.; Alberici, R. M.; Takiyama, M. M. K.; Huang, C. P. *Hazard. Ind. Wastes* **1994**, *26*, 230.
- (12) Nimlos, M. R.; Jacoby, W. A.; Blake, D. M.; Milne, T. A. *Photocatalytic Purification and Treatment of Water and Air*; Ollis, D. F., Al-Ekabi, H., Eds.; Elsevier Science Publishers: Amsterdam, 1993; p 387.
- (13) Yamazaki-Nishida, S.; Cervera-March, S.; Nagano, K. J.; Anderson, M.; Hori, K. *J. Phys. Chem.* **1995**, *99*, 15814.
- (14) Basu, P.; Ballinger, T. H.; Yates, J. T., Jr. *Rev. Sci. Instrum.* **1988**, *59*, 1321.
- (15) (a) Miller, T. M.; Grassian, V. H. *J. Am. Chem. Soc.* **1995**, *117*, 10969. (b) Driessen, M. D.; Grassian, V. H. *J. Catal.* **1996**, *161*, 810.
- (16) Tanaka, K.; White, J. *J. Phys. Chem.* **1982**, *86*, 4708.
- (17) Berry, M. J. *J. Chem. Phys.* **1974**, *61*, 3114.
- (18) Bernstein, H. J. *Can. J. Res.* **1949**, *28B*, 132.
- (19) Hannus, I.; Kiricsi, I.; Tasi, G.; Fejes, P. *Appl. Catal.* **1990**, *66*, L7.
- (20) Miyake, A.; Nakagawa, I.; Miyazawa, T.; Ichishima, I.; Shimanouchi, T.; Misushima, S. *Spectrochim. Acta* **1958**, *13*, 161.
- (21) NIST Standard Reference Database 69, Aug 1997.
- (22) Little, L. H. *Infrared Spectra of Adsorbed Species*; Academic: New York, 1966.
- (23) Davydov, A. A. *Infrared Spectroscopy of Adsorbed Species on the Surface of Transition Metal Oxides*; Wiley and Sons: Chichester, 1990.
- (24) Saussy, J.; Lavalley, J.-C.; Bovet, C. *J. Chem. Soc., Faraday Trans. I* **1982**, *78*, 1457.
- (25) Bocuzzi, F.; Ghiotti, G.; Chiorino, A. *Surf. Sci.* **1985**, *162*, 361.
- (26) Hwang, S.-J.; Petucci, C.; Raftery, C. *J. Am. Chem. Soc.* **1997**, *119*, 7877.
- (27) Sanhueza, E.; Hisatsune, I. C.; Heicklen, J. *Chem. Rev.* **1976**, *76*, 801.
- (28) Sanhueza, E.; Heicklen, J. *Int. J. Chem. Kinet.* **1974**, *6*, 553.
- (29) Bertrand, L.; Franklin, J. A.; Goldfinger, P.; Huybrechts, G. *J. Phys. Chem.* **1968**, *72*, 3926.
- (30) Huybrechts, G.; Meyers, L. *Trans. Faraday Soc.* **1966**, *62*, 2191.
- (31) Several experiments were done with C₂H₄ and C₂H₆ added to the gas mixture in order to trap chlorine atoms in the gas phase.
- (32) Larson, S. A.; Falconer, J. L. *Photocatalytic Purification and Treatment of Water and Air*, Ollis, D. F., Al-Ekabi, H., Eds.; Elsevier Science Publishers: Amsterdam, 1993; p 473.